

# Performance limitations of a Y-branch directional-coupler-based polymeric high-speed electro-optical modulator

Qingjun Zhou

Jianyi Yang

Zhong Shi

Yongqiang Jiang

Brie Howley

Ray T. Chen, FELLOW SPIE

University of Texas at Austin

Microelectronic Research Center

Austin, Texas 78712

E-mail: raychen@uts.cc.utexas.edu

**Abstract.** To find the optimal driving voltage and bandwidth for electro-optic polymer-waveguide-based directional couplers, four electrode structures are investigated. They are the microstrip line (MSL), the asymmetric coplanar waveguide with ground (ACWG), the coplanar waveguide with ground (CPWG), and the edge-coupled microstrip line (CMSL). UV15:Polymethyl methacrylate/dispersed-red 1:UV11-3-based directional couplers are evaluated. The CPWG and the ACWG have almost the same driving voltages, which are about twice the driving voltage of the CMSL. The MSL has the largest driving voltage, which is 20 to 25% higher than the driving voltages of the CPWG and ACWG. Simulation results further conclude that the MSL has the largest bandwidth, and its bandwidth is about 1.6 times that of the bandwidth of the CMSL, which has the narrowest bandwidth. The bandwidths of the ACWG and CPWG are 1.4 and 1.2 times that of the CMSL, respectively. The driving voltages for the four different devices are experimentally confirmed. © 2004 Society of Photo-Optical Instrumentation Engineers. [DOI: 10.1117/1.1666865]

Subject terms: electro-optic modulator; directional coupler; traveling-wave electrode.

Paper 030423 received Aug. 29, 2003; accepted for publication Oct. 31, 2003.

## 1 Introduction

High-speed electro-optic (EO) modulators have been widely used in many commercial and military applications. Recently, EO polymers have attracted extensive attention as materials with which to build modulators, because of their advantages over inorganic materials. These advantages include: 1. low dispersion in the index of refraction between infrared and millimeter-wave frequencies, and 2. potential for optoelectronic integration due to polymers' processing flexibility. Successful high-speed EO-polymer-based Mach-Zehnder modulators have been demonstrated.<sup>1</sup> In a Mach-Zehnder modulator, a direct-current (dc) bias is required to set the modulator at the half-power point, resulting in more complicated circuit fabrication; meanwhile, the dc drift phenomenon can cause serious nonlinear distortion of the transfer curve for analog systems such as CATVs and phased-array antennas. These problems may be avoided or alleviated by using modulators based on properly designed directional coupler structures.<sup>2</sup> A modulator based on a  $1 \times 2$  Y-branch directional coupler in which the input ends of the two waveguides are linked by a Y-branch, as shown in Fig. 1, can avoid dc bias, since this modulator is automatically set to the half-power point due to the 3-dB splitter. The high-linearity, low-intermodulation-distortion, and other unique characteristics of this kind of modulator are theoretically investigated in Ref. 3. An et al.<sup>2</sup> demonstrated a polymer-based Y-branch directional coupler with lumped electrodes. However, to achieve high-speed modulation, a traveling-wave electrode is essential. The structures of this

kind of traveling-wave electrode, which is generally applicable to directional-coupler-based polymeric EO modulators, are further explored in this work.

For an EO-polymer-based high-speed directional coupler, the task of the traveling-wave electrode is to generate an electrical field whose vertical components are different in the two parallel optical waveguides. This field difference induces a difference between the effective indexes of the two waveguides, and thus modulates the output optical intensities. For an EO-polymer-based high-speed Mach-Zehnder (MZ) modulator, the traveling-wave electrode is usually a microstrip line. The bottom electrode of the microstrip line is necessary for the poling process. When the EO-polymer layer is uniformly poled in the vertical direc-

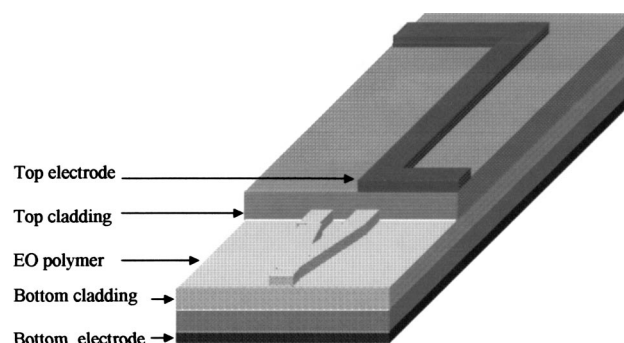


Fig. 1 Schematic of EO-polymer-based directional coupler with microstrip line.

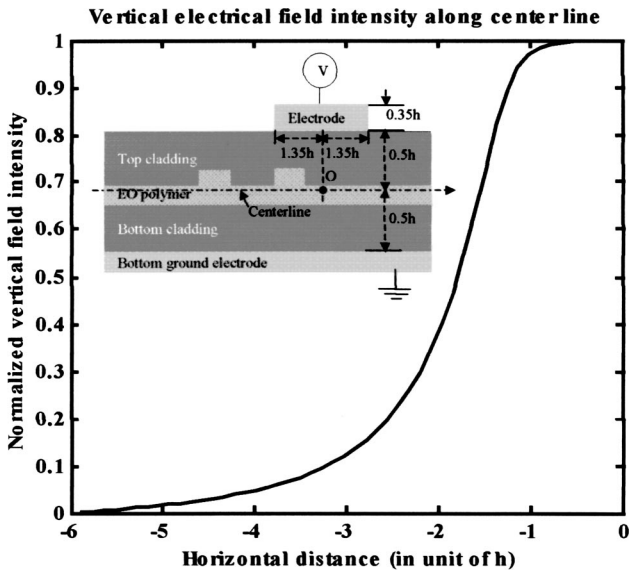


Fig. 2 Vertical electrical field distribution along the centerline of the polymer layers (including bottom cladding, EO polymer layer, and top cladding). The microstrip line that generated this field is also shown in the figure. (The original point of the horizontal distance axis corresponds to the “O” point shown in the picture).

tion, the microstrip line is usually only applied to one of the two arms of the MZ modulator. The electrode-induced electrical field in the other arm is almost zero, since the separation between the two optical arms of an MZ modulator is much larger than the polymer layer (including bottom cladding, active EO polymer layer, and top cladding) thickness (denoted by “h”). However, the situation is quite different for polymer-based directional couplers, since their optical waveguide separations are comparable to their polymer layer thickness, which is  $\sim 10 \mu\text{m}$  including top and bottom claddings. Figure 2 shows a microstrip line’s electrical field intensity (vertical component only) along the centerline of the polymer layers. The microstrip line that generated this electrical field is also shown in the same figure. In this figure, all the lengths are denoted in unit of the polymer-layer thickness (h) and the electrical field intensity

is normalized. The electrical field shown in Fig. 2 is obtained by solving the Poisson equation. The dielectric constants of the polymers (including bottom cladding, EO layer, and top cladding) are equal to 2.40 in the calculation. Based on this figure, it is obvious that if the optical waveguide separation is comparable with the polymer-layer thickness, the difference between the vertical electrical fields in the two optical waveguides cannot be large. Since the modulated signal is proportional to the electrode-induced vertical-electrical-field difference, and the microstrip line cannot effectively induce such a field difference, the microstrip line is not a very efficient traveling-wave electrode structure for polymer-based directional couplers, and it is worthwhile to explore other electrode structures. To find the optimal traveling-wave electrode formation for EO-polymer-based directional couplers, four electrode structures, as shown in Fig. 3, are evaluated and compared in this work by calculating the modulators’ driving voltages and bandwidths, and by experimentally measuring their performance features. The four structures are: 1. microstrip line (MSL), 2. asymmetric coplanar waveguide with ground (ACWG), 3. coplanar waveguide with ground (CPWG), and 4. edge-coupled microstrip line (CMSL).

In Sec. 2, the polymer materials used to fabricate the optical waveguides are introduced and the waveguides are designed. In Sec. 3, the traveling-wave electrode structures are described and the electrode dimensions that satisfy the  $50\Omega$ -characteristic-impedance requirements are obtained using the finite-element method. Section 4 gives the evaluation method and results for the driving voltage and bandwidth for modulators with different electrode structures. Section 5 presents the device fabrication and the driving voltage measurement results. Conclusions are given in the last section.

## 2 Optical Waveguide Materials and Structure

### 2.1 Materials

Polymethyl methacrylate (PMMA) doped with dispersed red 1 chromophore (DR1) is chosen as the representative for EO polymers to explore the optimal electrode design. DR1/PMMA has been widely used to fabricate EO-

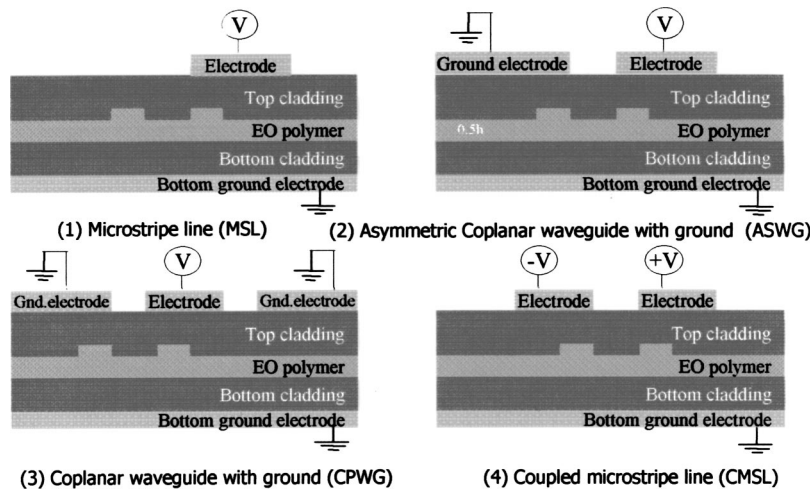


Fig. 3 Schematic of traveling-wave electrodes for EO-polymer-based directional couplers.

**Table 1** Waveguide materials and parameter. Waveguide separation refers to the distance between the inner edges of the two optical channels.

WG No.	Bottom cladding			EO polymer layer				Top cladding			Effective index	
	Material	Index	Thick ( $\mu\text{m}$ )	Material	Index	Thick ( $\mu\text{m}$ )	Rib depth ( $\mu\text{m}$ )	Waveguide separation ( $\mu\text{m}$ )	Material	Index		Thick ( $\mu\text{m}$ )
1	UV15	1.50	4.0	DR1/PMMA	1.55	4.0	1.44	13.0	UV11-3	1.51	4.0	1.54

polymer-based devices and it is commercial available. UV15 and UV11-3 are the bottom cladding and top cladding materials, respectively. The refractive indexes at 1.55  $\mu\text{m}$  of these materials are listed in Table 1. Note that all the data and results given in this work are for transverse magnetic (TM) mode at 1.55- $\mu\text{m}$  wavelength.

## 2.2 Waveguide Structure

Although the traveling-wave electrodes discussed in this work should be generally valid for polymeric EO modulators based on any directional coupler structures where the two optical waveguides are coplanar, the  $1 \times 2$  Y-branch directional coupler<sup>2</sup> is chosen here as an example.

The optical waveguides are rib channels as shown in Fig. 3. The rib depth and width are calculated using the effective index method (EIM). The single-mode condition for large cross section rib waveguides is used to assure that only one TM mode is formed in the waveguides.<sup>4-6</sup>

The interaction length is set to be 2.0 cm to optimize the performance, which is delineated in this work. The beam propagation method is used to search a proper waveguide separation, with which the conversion length is around 2.8 cm, which is around  $\sqrt{2}$  times of the interaction length. In this case, one arm of the  $1 \times 2$  Y-branch directional coupler can be switch off using the lowest driving voltage. All related parameters of the optical waveguide are listed in Table 1.

## 3 Electrode Structures

As shown in Fig. 3, four electrode structures are candidates for directional-coupler-based polymeric modulators. The electrode dimensions, which satisfy the  $50\Omega$ -characteristic-impedance requirement, are calculated using the finite element method. In these calculations, the polymers' dielectric constants are assumed equal to the square of their refractive indexes. The electrode's conductivity is set to be  $4.1$

$\times 10^7$  S/m for gold. The calculated electrode dimensions and characteristic parameters are given in Table 2.

## 4 Electrode Structure Optimization

In this section, the four traveling-wave electrode structures are compared in terms of the driving voltage and bandwidth of the modulators using these electrodes. The evaluation methods and results for driving voltages and bandwidths are described next.

### 4.1 Driving Voltage

In these four modulators, the left edge of the right optical waveguide is located 0.5- $\mu\text{m}$  right, corresponding to the left edge of the active electrode. The modulation curves of these modulators can be calculated using the beam propagation method. The detailed calculation steps are listed here.

1. For a given applied voltage, the Poisson equation is solved to derive the electrical field distribution.
2. The index changes of TM modes are calculated using  $\Delta n = -0.5n^3\gamma_{33}E$ , where  $n$  is the EO polymer's refractive index,  $\gamma_{33}$  is the EO efficient, and  $E$  is the electrical field in the vertical direction.
3. The output optical intensity is calculated using the beam propagation method based on the index distribution obtained in the second step.
4. Change driving voltage value and repeat steps 1, 2, and 3.

Figure 4 gives the modulation curves of modulators with different electrode structures. In these calculations,  $\gamma_{33}$  of DR1/PMMA is equal to 10 pm/v (these values have been successfully achieved in our experiments). A discussion on the simulation results of driving voltages is given in Sec. 5.2.

**Table 2** Electrode parameter.

Polymer material	Electrode structure	Polymer thickness ( $\mu\text{m}$ )	Top electrode thickness ( $\mu\text{m}$ )	Bottom electrode thickness ( $\mu\text{m}$ )	Active electrode width ( $\mu\text{m}$ )	Electrode gap ( $\mu\text{m}$ )	Effective index	Conductor loss (dB/cm/ $\sqrt{\text{GHz}}$ )
UV15:	MSL	12.0	3.0	2.4	35.0	12.0	1.43	0.251
DR1/PMMA:	ACWG	12.0	3.0	2.4	33.0	12.0	1.41	0.259
UV11-3	CPWG	12.0	3.0	2.4	31.0	12.0	1.38	0.271
	CMSL	12.0	3.0	2.4	26.0	12.0	1.35	0.275

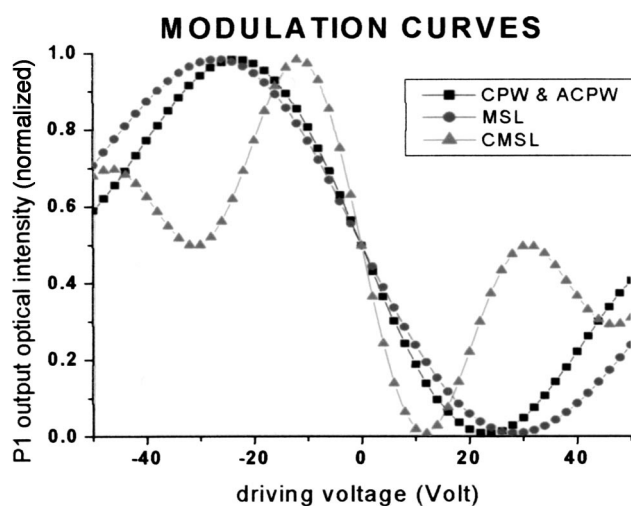


Fig. 4 Modulation curves of UV15:PMMA/DR1:UV11-3-based  $1 \times 2$  Y-branch directional couplers with different electrode structures.

#### 4.2 Bandwidth

The bandwidth is estimated using the small-signal analysis method reported in Ref. 7. Based on Eq. (22) in Ref. 7, as well as the optical refractive index, the microwave refractive index, and the attenuation constant obtained in Sec. 3, the frequency responses of the directional coupler are derived. Figure 5 shows the calculated frequency responses of  $1 \times 2$  Y-branch directional couplers for UV15:DR1/PMMA:UV11-3. The different lines in this figure correspond to the couplers with different electrode structures. The calculated 3-dB bandwidths of DR1 modulators with different electrode structures are 86.3 GHz (MSL), 72.8 GHz (ACWG), 63.0 GHz (CPWG), and 52.3 GHz (CMSL), respectively.

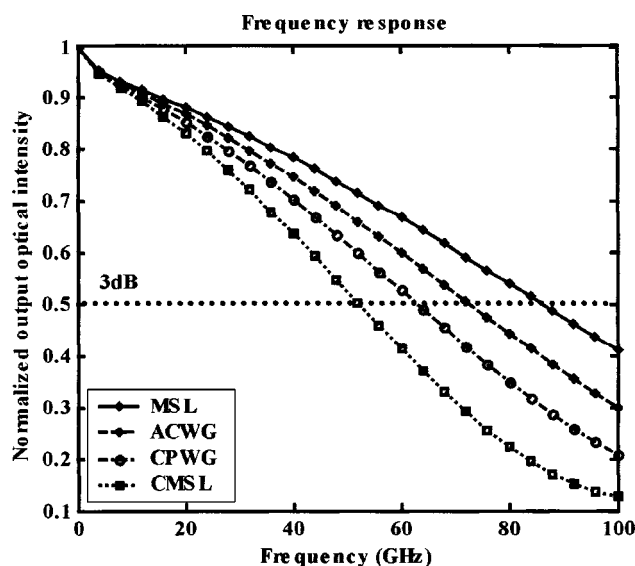


Fig. 5 Frequency responses of UV15:PMMA/DR1:UV11-3-based  $1 \times 2$  Y-branch directional couplers with different electrode structures.

## 5 Device Fabrication and Test

The modulators described in the previous sections are fabricated and their driving voltages are tested.

### 5.1 Fabrication

The fabrication steps are as follows.

1.  $3\text{-}\mu\text{m}$  Al is deposited on silicon wafers.
2. UV15 is diluted by cyclopentanone, then a thin layer of UV15 is spin coated and UV cured to serve as the bottom cladding.
3. DR1/PMMA is dissolved into cyclopentanone and then the solution is used to spin coat the EO polymer layer.
4. A normal photolithography process is used to pattern the optical waveguide.
5. Waveguides are etched using reactive ion etching (RIE) with oxygen and nitrogen.
6. An UV11-3 layer is coated and UV cured to serve as the top cladding.
7. A  $0.5\text{-}\mu\text{m}$  Al layer is deposited on top of the top cladding to serve as both the poling electrode and the top electrode.
8. The samples are poled for 30 min using 1100 V voltage.
9. The top electrodes are patterned using photolithography.
10. The samples are cleaved and ready for test.

### 5.2 Test

The fabricated modulators are tested at  $1.55\ \mu\text{m}$  using a Santec ECL-200 laser (Santec Corp., Hackensack, NJ). The input single-mode fiber is aligned to the waveguide, and the output is collected by a  $40\times$  objective lens and coupled to a photodetector. A fiber optical polarization controller is used to adjust the input polarization to TM.

To obtain the driving voltages of different electrode structures, an array of modulators with different electrode structures is fabricated on each chip. The switch voltage  $V_s$  is measured by applying a 1-KHz signal. Figures 6(a), through 6(d) show the modulation and the modulated signals of four modulators with different electrode structures. In each figure, the sinusoidal curve is the modulation signal (electrical), the other curve with more curvatures is the modulated signal (optical), the horizontal axis is the time axis ( $200\ \mu\text{sec}$  per division), and the vertical direction shows the voltage for the modulation signal (10 V per division) and the optical intensity for the modulated signal. These measurements show that the switch voltages of the modulators under test are 24 V for the CMSL, 48 V for the ACWG and CPWG, and 60 V for the MSL. Although the measured switch voltages from different Si wafers have variations, the ratios between the measured switch voltages of the modulators with different electrode structures obtained from the same Si wafer are fixed. The ratios between the measured switch voltages of the modulators with different electrode structures are  $1(\text{CMSL}):2(\text{ACWG}):2(\text{CPWG}):2.5(\text{MSL})$ .



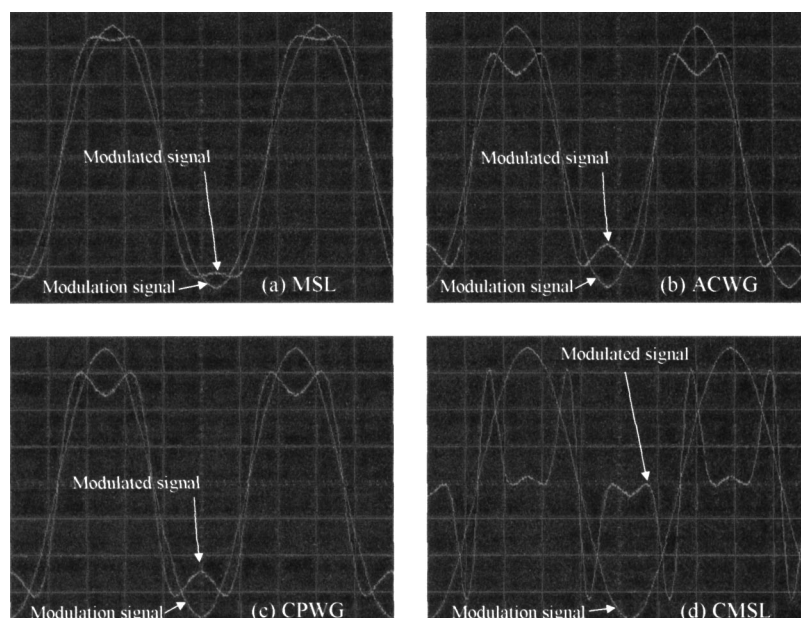


**Fig. 6** Measured modulation and modulated signals of UV15:PMMA/DR1:UV11-3-based  $1 \times 2$  Y-branch directional couplers with different electrode structures: (a) MSL, (b) ACWG, (c) CPWG, and (d) CMSL.

The ratios between the driving voltages of different electrode structures agree well with the simulation results given in Sec. 4.1. Both the experimental and simulation results show that using CMLs, CPWGs, or ACWGs can reduce the driving voltages. The CMSL is the best electrode structure in terms of the driving voltage. When the electrodes' top electrode separations are the same and have a value similar to the polymer layer thickness, the CMSL's driving voltage is only half of that of the CPWG or the ACWG. The CPWG and the ACWG have almost the same driving voltage. The MSL has the largest driving voltage that is 20 to 25% higher than the driving voltages of the CPWG and ACWG. Further experimental results on bandwidth will be presented in a separate publication.

## 6 Conclusions

For electrodes with the same top electrode separations, a directional-coupler-based modulator with a CMSL has the lowest driving voltage, but its bandwidth is also the smallest. A modulator with a MSL has the largest driving voltage and the largest bandwidth. The driving voltage of a modulator with a CPWG is almost the same as that of a modulator with an ACWG. A modulator with a CPWG has smaller bandwidth compared with that of a modulator with an ACWG. The experimental results for the driving voltage agree with the modeling results.

The results obtained in this work indicate a tradeoff between the driving voltages and the bandwidths. Different electrode structures may be suitable for different applications. If the EO polymer has a relatively smaller EO coefficient and the driving voltage is a critical concern, the CMSL is the best choice. On the other hand, if the EO polymer has a relatively larger EO coefficient or the bandwidth is the critical concern, the MSL may be the best choice. The CPWG and ACWG are good for normal cases,

since their driving voltages are around 25% lower than that of a MSL and their bandwidths are 20 to 40% larger than that of a CMSL.

## Acknowledgments

This research is supported by AFOSR, MDA, DARPA, IBM, Omega Optics, and the ARP/ATP program of Texas State.

## References

1. D. Chen, D. Bhattacharya, A. Udupa, B. Tsap, H. R. Fetterman, A. Chen, S. S. Lee, J. Chen, W. H. Steier, and L. R. Dalton, "High-frequency polymer modulators with integrated finline transitions and low  $V_{\pi}$ ," *IEEE Photonics Technol. Lett.* **11**(1), 54–56 (1999).
2. D. An, Z. Shi, L. Sun, J. M. Taboada, Q. Zhou, X. Lu, R. T. Chen, S. Tabg, H. Zhang, W. H. Steier, A. Ren, and L. R. Dalton, "Polymeric electro-optic modulator based on  $1\lambda/2$  Y-fed directional coupler," *Appl. Phys. Lett.* **76**(15), 1972–1974 (2000).
3. R. F. Tavlykaev and R. V. Ramaswamy, "Highly linear Y-fed directional coupler modulator with low intermodulation distortion," *J. Low Temp. Phys.* **17**(2), 282–291 (1999).
4. R. A. Soref, J. Schmidtchen, and K. Petermann, "Large single-mode rib waveguides in GeSi-Si and Si-on-SiO<sub>2</sub>," *IEEE J. Quantum Electron.* **27**(8), 1971–1974 (1991).
5. S. P. Pogossian, L. Vescan, and A. Vonsovici, "The single-mode condition for semiconductor rib waveguides with large cross section," *J. Low Temp. Phys.* **16**(10), 1851–1853 (1998).
6. U. Fisher, T. Zinke, J. R. Kropp, F. Arndt, and K. Petermann, "0.1 dB/cm waveguide losses in single-mode SOI rib waveguides," *IEEE Photonics Technol. Lett.* **8**(5), 647–648 (1996).
7. H. Chung and W. S. C. Chang, "Normal-mode small-signal analysis of traveling-wave directional couplers," *IEEE J. Quantum Electron.* **28**(5), 1353–1359 (1992).

**Qingjun Zhou** received his BS degree in physics from Jilin University, China, and MS in electrical and computer engineering (ECE) from the University of Texas at Austin. Now, he is working toward a PhD degree in ECE at the University of Texas at Austin. His research interests include high-speed electrooptic devices and phased array antennas.

**Jianyi Yang** received his PhD degree from Zhejiang University, Hangzhou, China, in 1996. Then he joined the faculty of Zhejiang University. From August 2000 to November 2002, he did postdoctoral research in the Microelectronics Research Center at the University of Texas at Austin. Now he is a professor of the Department of Information Science and Electronics Engineering, Zhejiang University. His research interests include optical waveguides and components, optical MEMS, and optical interconnects.

**Zhong Shi** received his BS in optics from Shandong University, and MS in fiber communications from Beijing University of Posts and Telecommunications. He is currently studying in the ECE department of the University of Texas at Austin for his PhD.

**Yongqiang Jiang** received his BS degree in physics in 1998 and his MS degree in optics in 2001, both from Fudan University in China. From 1998 to 2001, his research topic was nonlinear optical properties of II-VI semiconductor quantum wells with potential applications for lasers and other photonic devices operating in the blue-green region. Since 2001, he has been working toward a PhD degree in electrical engineering at the University of Texas at Austin. His current research interest is optically controlled, wide bandwidth phased-array antennas (PAAs). He has published approximately 20 technical papers since 2000.

**Brie Howley** received his BS degree from the University of Wisconsin-Madison in 1998. From 1998 to 2001, he worked for Mo-

torola's Semiconductor Product Sector on the discrete components research and development team. Since 2001, he has been working toward a PhD degree in electrical engineering in the area of plasma, optics, and quantum electronics at the University of Texas at Austin. His research topic is optically controlled, wide bandwidth phased-array antennas.

**Ray T. Chen** received his BS degree in physics from National Tsing-Hua University in 1980 in Taiwan, his MS degree in physics in 1983, and his PhD degree in electrical engineering in 1988, both from the University of California. He is the Temple Foundation Endowed Professor (1998-) in the Department of Electrical and Computer Engineering at the University of Texas (UT), Austin. He joined UT Austin as a faculty member to start an optical interconnect research program in the ECE department in 1992. Prior to his UT professorship, he was working as a research scientist, manager, and director in the Department of Electrooptic Engineering in the Physical Optics Corporation in Torrance, California, from 1988 to 1992, where he got his security clearance to work on a U.S. Marine-related project using holographic image displays as a decoy for heat seeking missiles. He holds 12 issued patents. He has chaired or been a program committee member for more than 50 domestic and international conferences organized by IEEE, SPIE, OSA, and PSC. He is a Fellow of SPIE, IEEE, and the Optical Society of America. He was the recipient of the 1987 UC Regent's dissertation fellowship and of the 2000 UT Engineering Foundation Faculty Award for his contributions in research, teaching, and services.